Acoustic Emission Analysis Coupled with Thermogravimetric Experiments Dedicated to High Temperature Corrosion Studies on Metallic Alloys

Eric SERRIS **, Omar AL HAJ **, Jean KITTEL *, Véronique PERES **,
Francois GROSJEAN *, Francois ROPITAL *, Michel COURNIL**
* IFP Energies nouvelles, BP3 rond-point de l'échangeur de Solaize, 69360 Solaize, France
** Ecole Nationale Supérieure des Mines de Saint-Etienne, Saint-Etienne, France

Abstract. High temperature corrosion of metallic alloys (like iron, nickel, zirconium alloys) can damage equipment of many industrial fields (refinery, petrochemical, nuclear …). Acoustic emission (AE) is an interesting method owing to its sensitivity and its non-destructive aspect to quantify the level of damage in use of these alloys under various environmental conditions. High temperature corrosive phenomena create stresses in the materials; the relaxation by cracks of these stresses can be recorded and analyzed using the AE system. The goal of our study is to establish an acoustic signals database which assigns the acoustic signals to the specific corrosion phenomena. For this purpose, thermogravimetric analysis (TGA) is coupled with acoustic emission (AE) devices.

The oxidation of a zirconium alloy, zircaloy-4, is first studied using thermogravimetric experiment coupled to acoustic emission analysis at 900°C. An inward zirconium oxide scale, preliminary dense, then porous, grow during the isothermal isobaric step. The kinetic rate increases significantly after a kinetic transition (breakaway). This acceleration occurs with an increase of acoustic emission activity. Most of the acoustic emission bursts are recorded after the kinetic transition. Acoustic emission signals are also observed during the cooling of the sample. AE numerical treatments (using wavelet transform) completed by SEM microscopy characterizations allows us to distinguish the different populations of cracks.

Metal dusting represents also a severe form of corrosive degradation of metal alloy. Iron metal dusting corrosion is studied by AE coupled with TGA at 650°C under C_4H_{10} + H_2 + He atmosphere. Acoustic emission signals are detected after a significant increase of the sample mass.

Introduction

Over the last few decades several authors have been studying high temperature corrosion behavior of metals and alloys, steels sulfidation [1], metal dusting inhibition [2], and alloys oxidation [3] using the acoustic emission devices. Since 1977 other authors have coupled acoustic emission with thermogravimetric analysis (TGA) in order to improve the knowledge of different high temperature corrosion phenomena [4-8]. The sample mass variation and the AE signals were simultaneously recorded over these experiments. In this

study, we use an innovative device to perform such experiments that is based on TGA analysis coupled with in situ acoustic emission. The technique is applied to study mass variation and AE signals during the oxidation at high temperature of a zirconium alloy, Zircaloy-4 and also during metal dusting of pure iron.

1 Experimental

The experiments are performed on Zircaloy-4 platelet specimens (4.8 mm x 4.6 mm x 0.5 mm) and iron platelet (4.4 mm x 4.6 mm x 1 mm). The chemical compositions of these materials are given in Table 1 and 2. Samples are polished and cleaned with acetone and ethanol before the oxidation tests.

Table 1: Chemical composition of Zircaloy-4 in weight% or ppm

Sn (wt%)	Fe (wt%)	O (wt%)	Cr (wt%)	C (wt ppm)	Nb (wt ppm)	H (wt ppm)	Zr
1.32 – 1.35	0.21	0.123 – 0.129	0.11	125 -140	< 40	< 3	Bal.

Table 2: Chemical composition of pure iron in ppm

Fe	C	Cr	Si	Al	Ti	Mo
+99,8%	2 ppm	0,94 ppm	0,18 ppm	0,19 ppm	0,05 ppm	0,03 ppm

Thermogravimetric analyses are carried out on a symmetric thermobalance (SETARAM TAG 24) with Pt-Rh 6%/ Pt-Rh 30% thermocouples, in order to measure the specimen's mass change during the oxidation tests with a precision of ± 0.001 mg.
For Zy-4 oxidation test the temperature is fixed at 900°C ± 0.1°C (this temperature is in the field of accidental conditions in the nuclear power plants); the heating rate is 15°C/min in pure helium. The isothermal dwell time is fixed to 5 hours. Once the desired temperature is reached (T = 900°C), helium is switched to a mixture of (75% He + 21% O_2 + 4% N_2) for the first series of oxidation tests. Another oxidant gas mixture (80% He + 20% O_2) is used for the second series of oxidation tests. In both series the oxidant gas is introduced by mass flow meters with a total gas flow rate of 50 ml/min. The cooling rate is 15°C/min under the same process gas mixture.

For iron metal dusting tests the temperature is fixed at 650°C ± 0.1°C ; the heating rate is 15°C/min in pure helium. The isothermal dwell time is fixed to 24 hours. Once the desired temperature is reached, helium is switched to a mixture of (90% He + 5 % iC_4H_{10} + 5 % H_2). The reactive gases are introduced by mass flow meters with a total gas flow rate of 50 ml/min. The cooling rate is 15°C/min under helium.

AE piezoelectric sensors are linked to the waveguide via a metallic support; sensors and metallic support are placed inside the cold part of the thermobalance where the temperature does not exceed 150°C. The sensors are linked to an acquisition chain controlled by the AEwin™ software and data are analyzed using Noesis™ software provided by the Physical Acoustics Corporation Company. The characteristics of the acquisition chain are given in Table 3. The threshold is very low fixed to 18 dB_{AE}.

Table 3 : Main characteristics of the AE acquisition chain

Instrumentation	Sensors	Threshold (dB_{AE})	System filter (KHz)	Model of the amplifier	Sampling rate	PDT - HDT - HLT
Characteristics	PICO 30	18	10 - 1200	2/4/6 gain : 60 dB_{AE}	0.25 µs (4MHz)	100 - 200 - 400 (µs)

Discontinuous acoustic emission analysis (AE burst) is used during this study. At ambient temperature, the normalized Hsu-Nielsen test is carried out to verify the AE system.

Blank tests at 900°C under air or oxygen without any specimen are carried out to validate that the waveguide did not significantly react with the gas mixture. During these tests, the stability of the mass signal confirm the chemical inertness of the waveguide.

2. Results

Blank tests allow us to distinguish the acoustic emission signals which result from the instrumental noise (IN). They are characterized by a very short duration and a low number of counts, 95% of these bursts are characterized by 1 count and a duration of 1 µs. They are also characterized by a high average frequency in the range of 200 kHz to 1000 kHz including the resonance frequency of the sensors (300 kHz). Burst's absolute energy is very low and doesn't exceed 0.1 aJ/burst. These instrumental noise AE bursts are deleted from the acoustic emission analysis for the rest of the study.

2.1 Zircaloy-4 corrosion

2.1.1 Oxidation tests under air

Figure 1 shows the bursts amplitude recorded during the oxidation tests in parallel with the kinetic rate variation as function of time. According to the kinetic rate curves, we note that AE bursts have been recorded just after the kinetic transition (breakaway) occurring 2 400 s (40 minutes) after the introduction of the oxidant gas mixture [9-10]. Each time an important AE activity appears just after the breakaway. These bursts are called post-transition bursts. Post-transition bursts recorded during the temperature dwell time are characterized by mean amplitude in the range of 18 to 40 dB_{AE}. AE bursts possess a low average frequency varying between 1 kHz to 200 kHz. Their absolute energy average is about 10 aJ/burst. AE signals are also recorded during the cooling of the sample. AE bursts recorded during the cooling step are more energetic (100 aJ/burst) and characterized by long duration (1000 µs/burst), and high counts number/burst (300 counts/burst as an average).

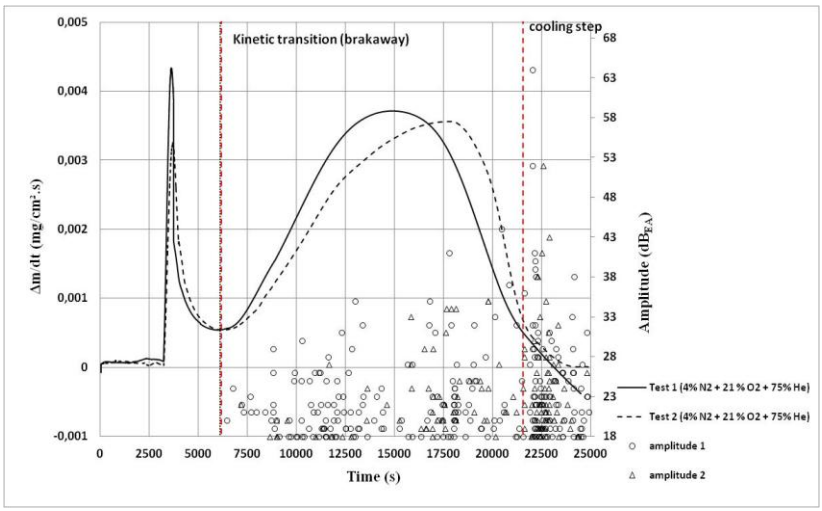

Fig. 1. Rate of mass gain and burst amplitude as a function of time during Zircaloy-4 oxidation tests under 75% He + 21% O2 + 4% N2

SEM cross section of oxidized sample (Figure 2) obtained with scanning electron microscopy (JEOL 6500 F) indicates that cracks are located inside the inward zirconia layer. Cracks are visible in the external dense zirconia layer (type1), well distributed thin and convoluted cracks are observed parallel to the metal oxide interface (type 2) and big open cracks are periodically observed perpendicular to this interface totally crossing the zirconia layer (type 3). The core of the sample remains partially oxidized forming α-ZrO solid solution of oxygen in zirconium according to the Zirconium- Oxygen binary diagram [11].

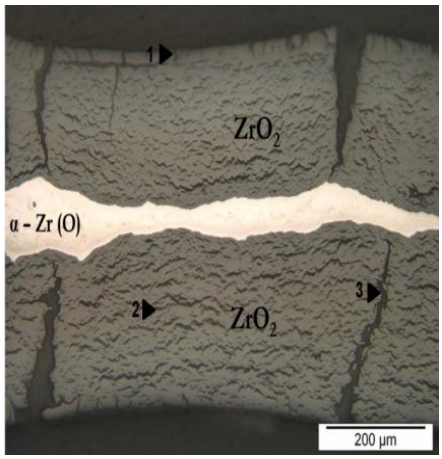

Fig. 2. SEM cross section of Zircaloy-4 oxidized under air at 900°C

Theses cracks can be associated with the AE signals recorded after the kinetic transition. We can attribute the AE bursts to these post-transition stage cracks. Even the AE threshold is low (18 dB_{AE}), the type 2 convoluted cracks parallel to the metal/oxide interface probably do not generate AE signals. The number of type 2 cracks surpasses the amount of AE bursts which have been recorded during the oxidation test. These cracks seem not to be emissive events. This hypothesis needs some more investigations to be validated.

2.1.2. Oxidation tests under oxygen

The kinetic transition doesn't appear during the oxygen test without nitrogen (80% He + 20% O_2), the kinetic rate decreases or remains constant throughout the experiment (Figure 3). In order to confirm the absence of the kinetic transition under oxygen at 900°C, the dwell time was extended from 5 hours to 10 hours (Figure 3). Results obtained during the extended test (10 hours dwell time) confirm the absence of kinetic transition during the oxidation under oxygen. The kinetic oxidation under oxygen is defined by a sub-parabolic law. The oxidation process is governed by the oxygen vacancy diffusion through a dense zirconia layer.

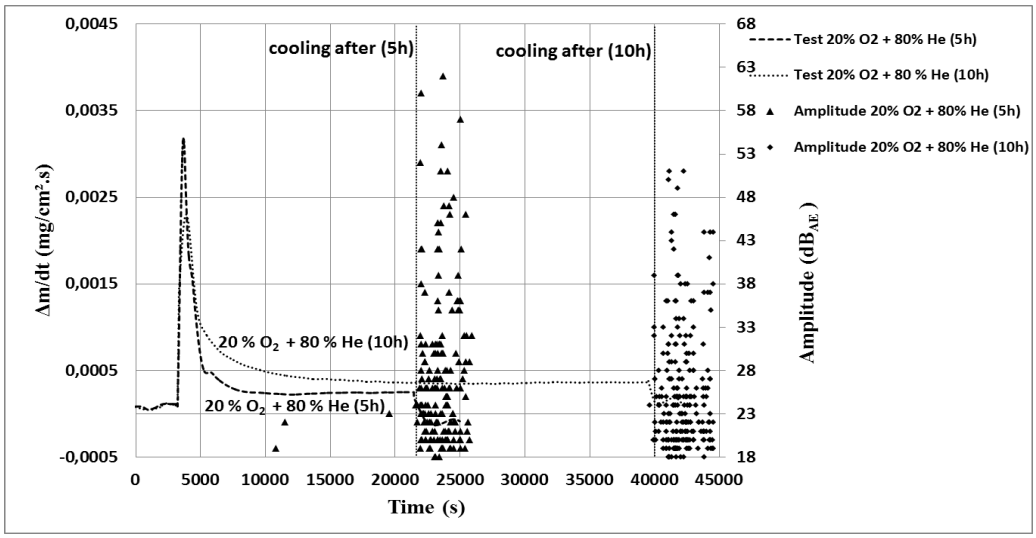

Fig.3. Rate of mass gain as a function of time and bursts amplitude variation during Zircaloy-4 oxidation tests under oxygen (▲) [5 hours] - (♦) [10 hours]

No kinetic transition and no AE signals are observed during the dwell times. AE bursts recorded during short and extended tests under oxygen appear only during the cooling step. The bursts parameters of these tests are similar (amplitude, counts number, duration, average frequency …). The AE bursts recorded during the cooling step are characterized by a high absolute energy (200 aJ/burst as average). Their counts' number is in the order of magnitude of hundreds of counts per burst, and their amplitude varying between 20 dB_{AE} and 60 dB_{AE}.

SEM cross section of oxidized samples under oxygen during 5 hours at 900°C (Figure 4) shows a very dense external zirconia layer. Cracks are only located in the α-Zr(O) scale, which is in white contrast in the metal phase close to the metal/oxide interface. The core of the sample is α-Zr which results from the transformation phase (β-Zr ➔ α-Zr) occurring during the cooling step for a temperature lower than 863°C.

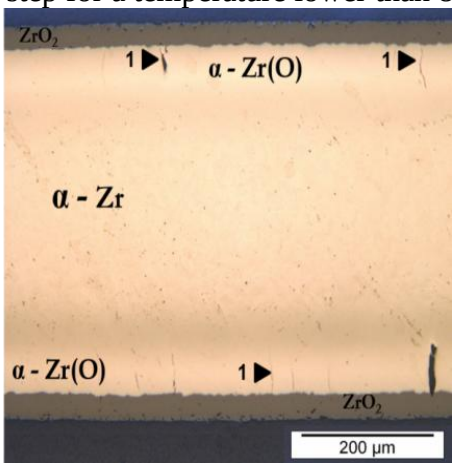

Fig. 4. SEM cross section of Zircaloy-4 oxidized 5 hours under oxygen at 900°C (cracks indicated by "1" indicators)

To study in detail the cooling AE signals, we applied a continuous wavelet analysis of their waveforms. AE bursts recorded during the cooling under air possess a wavelet different from that of AE signals recorded during the cooling under oxygen (Figure 5). AE burst waveform for air test is mainly punctual with one spots line localized between 280 kHz to 420 kHz (Figure 5.a). AE burst waveform for oxygen test is more continuous with two important spots lines; the first one is centred between 120 kHz to 180 kHz, the second one is located between 300 kHz to 450 kHz.

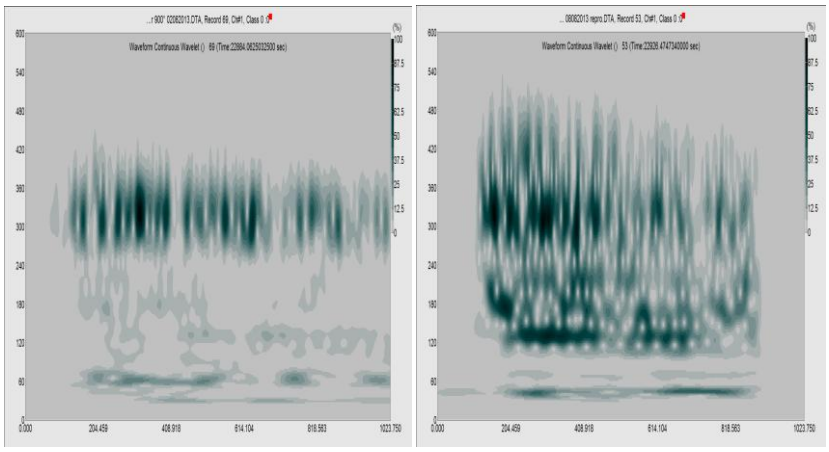

-a- -b-

Fig. 5. Typical AE burst waveform continuous wavelets recorded during the cooling of oxidation tests

For Zircaloy-4 oxidized samples under oxygen at 900°C, differences in thermal expansion coefficients of α-Zr, α-Zr(O) layer and ZrO2 dense scale during the cooling at temperature close to 400°C must be taken into account. Important compressive stresses can created cracks in α-Zr(O) layer (figure 4) which is sandwiched between the metal and the oxide. Considering the micrographs of oxidized samples under oxygen, the AE bursts observed during the last part of the cooling may be generated by the cracks observed in the α-Zr(O) layer.

2.2. Metal dusting

The sample mass gain of metal dusting tests on pure iron is shown as function of time in figure 6. The amplitude of acoustic bursts is also plotted in this figure. In the first part of the experiment (up to 40 000 s) the sample mass gain is slowly growing up to 1 mg. Then the sample mass gain accelerates and the curve becomes linear, the total mass gain is nearly 8 mg. Almost all of the mass gain comes from the carbon deposit at the sample surface. At the beginning of this linear part, the acoustic emission occurs until the end of the test.

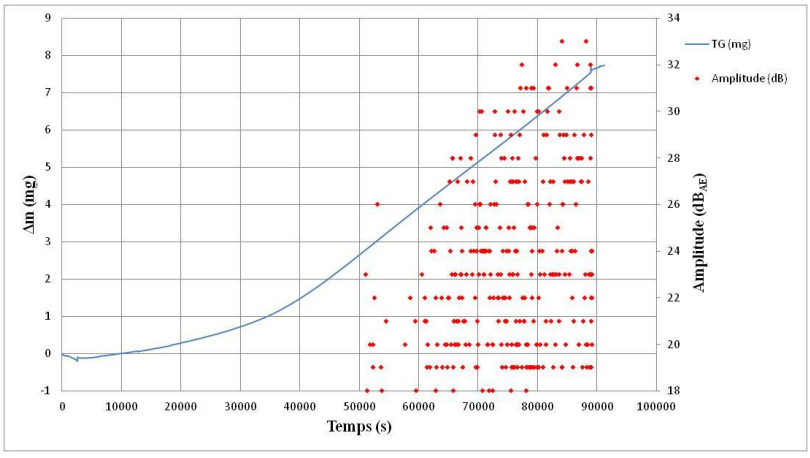

Fig. 6. Typical AE burst waveform continuous wavelets recorded during the cooling of oxidation tests

The metal dusting process can be described with several steps [12]. The first one is carbon dissolution inside the iron matrix. When the activity of carbon inside the iron reaches the activity of formation of cementite (Fe_3C), this phase can form according to this chemical reaction: $3\ Fe+C = Fe_3C$. When the surface is covered by cementite, a large amount of graphite and coke can deposit on the sample surface. Then the metastable cementite disintegrates by giving iron free particle and pits inside the iron matrix. We can

consider that the first step of the carbon dissolution is the slow part of mass gain curve and when the process of carbon and coke deposit (with cementite formation and disintegration) occurs, this corresponds to the linear part of the curve.
SEM cross section of the iron samples after 24 hours of metal dusting (Figure 7) shows the small carbons pits at iron surface.

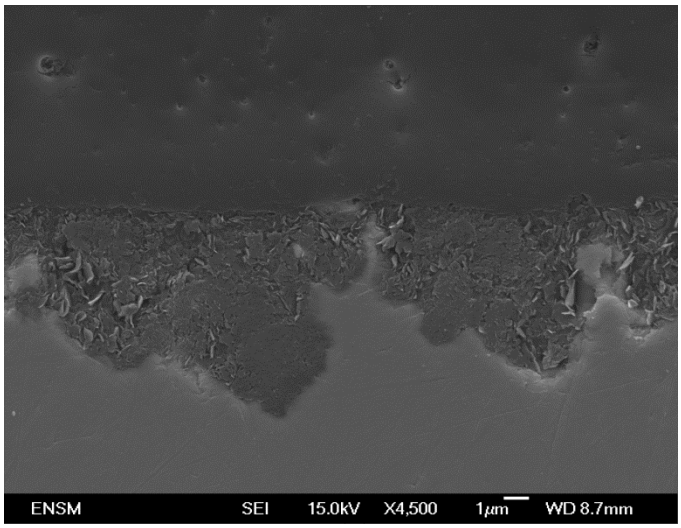

Fig. 7. SEM cross section of pure iron after 24 hours of metal dusting at 900°C

The darker zone of the sample surface is carbon enrichment inside the iron matrix. This hypothesis is confirmed by EDX plots throughout the surface.
To study in detail the AE signals, we apply a continuous wavelet analysis of their waveforms. We found that there is only one kind of wavelet for all bursts (figure 8).

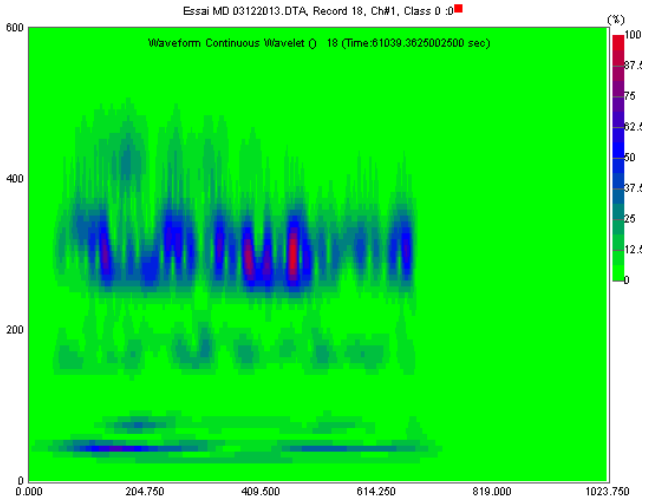

Fig. 8. Typical AE burst waveform continuous wavelets recorded during the metal dusting

The acoustic emission begins with the acceleration of sample mass gain (linear part of the curve after 50000 s of experiment). We consider that the most probable step that may lead to a significant energetic release is the decomposition of cementite and more precisely the incorporation of carbon inside the iron matrix. This non reversible step may lead to the acoustic emission recorded in our study.

3. Conclusions

Thermogravimetric experiments coupled with acoustic emission analysis are an interesting way to improve knowledge on the corrosion of metallic materials at high temperature. AE technique allows us to study in details the oxidation behaviour of zircaloy-4 at high temperature. The kinetic transition is detected under air tests at 900°C by a change in the rate of mass gain during the isothermal dwell time. This breakaway is also immediately detected by the AE activity. AE analysis is complementary of post-mortem oxidized samples characterizations. It allows us to distinguish the cracks which occur during the zircaloy-4 oxidation from the cracks which arise during the cooling of the samples. During the oxidation, the first cracks which appear after the breakaway are located in the external ZrO_2 layer perpendicular to the metal oxide interface. The AE signals correspond to these cracks. The numerous small convoluted thin pores observed deeper in the zirconia scale are not detected by the AE technique. Cracks due to cooling of oxidized samples under oxygen at 900°C are located in the α-Zr(O) phase. They possess a typical AE signature. From these studies we can conclude that mechanisms as diffusion of atoms (oxygen vacancies in case of zirconium inward oxidation in pure oxygen at 900°C) are not emissive. Irreversible mechanisms, as cracks initiation and propagation, generate AE signals.

We also successfully use this innovative device for petrochemical applications for which metal dusting represents a severe form of corrosion. Metal dusting of iron samples is studied by AE coupled with TGA at 650°C under isobutane and hydrogen. Acoustic emission signals are detected after a significant increase of the sample mass corresponding to carbon penetration in iron.

Acknowledgment

This work is a part of the French FUI program: IREINE (Innovation for REliability of INdustrial Equipments) dedicated to the development of devices and monitoring services to follow the corrosion of industrial process equipment. This program is founded by the French Rhone Alpes Region.

References

[1] M. Shuthe, A. Rahmel and M. Shütze, Oxidation of metals (1998) 33-70.
[2] F. Ferrer, J. Goudiakas, E. Andres and C. Brun, Nace Corrosion Conference, paper 01386 (2001)
[3] M.T. Tran, M. Boinet, A. Galerie, Y. Wouters, Corrosion Science, 52 (2010)2365–2371
[4] R.F. Hochman Proc. of the symp. On Properties of High Temperatures Alloys with Emphasis on Environnemental Effects (Eds. Z.A. Foroulis and F.S. Pettit). The Electrochemical Society (1977) 715
[5] M.J. Bennett, D.J. Buttle, P.D. Colledge, J.B. Price, C.B. Scruby and k.A. Stacey, Materials Science and Engineering, A120 199 (1989)
[6] H. J. Schmutzler and H.J. Grabke, Oxidation of metals, 39 (1992) 15- 29
[7] HJ. Grabke Materials and Corrosion; 1998 (49) 303
[8] F. Grosjean, J. Kittel, F. Ropital, E. Serris, V. Peres, Spectra Analyse 279 (2011), 35-44
[9] M. Tupin, M. Pijolat, F. Valdivieso, M. Soustelle Journal of Nuclear Materials; 342 (2005) 108-118
[10] M. Steinbrück, Journal of Nuclear Materials; 2014 (447) 46-55
[11] J.P. Abriata, J. Garcés, R. Versaci «The O-Zr (Oxygen-Zirconium) system », Bulletin of Alloy Phase Diagrams, 7-2, (1986),116-121
[12] D. J. Young, J. Zhang, C. Geers and M. Schutze, Materials and Corrosion, 62 (2011), 7-28